CrossMark

ORIGINAL PAPER

Constrained Spherical Deconvolution Tractography Reveals Cerebello-Mammillary Connections in Humans

Alberto Cacciola [1] · Demetrio Milardi [1,2] · Alessandro Calamuneri [3] · Lilla Bonanno [2] · Silvia Marino [2] · Pietro Ciolli [1] · Margherita Russo [2] · Daniele Bruschetta [1] · Antonio Duca [1] · Fabio Trimarchi [1] · Angelo Quartarone [1,2] · Giuseppe Anastasi [1]

Abstract According to the classical view, the cerebellum has long been confined to motor control physiology; however, it has now become evident that it exerts several non-somatic features other than the coordination of movement and is engaged also in the regulation of cognition and emotion. In a previous diffusion-weighted imaging-constrained spherical deconvolution (CSD) tractography study, we demonstrated the existence of a direct cerebellum-hippocampal pathway, thus reinforcing the hypothesis of the cerebellar role in non-motor domains. However, our understanding of limbic-cerebellar interconnectivity in humans is rather sparse, primarily due to the intrinsic limitation in the acquisition of in vivo tracing. Here, we provided tractographic evidences of connectivity patterns between the cerebellum and mammillary bodies by using whole-brain CSD tractography in 13 healthy subjects. We found both ipsilateral and contralateral connections between the mammillary bodies, cerebellar cortex, and dentate nucleus, in line with previous studies performed in rodents and primates. These pathways could improve our understanding of cerebellar role in several autonomic functions, visuospatial orientation, and memory and may shed new light on neurodegenerative diseases in which clinically relevant impairments in navigational skills or memory may become manifest at early stages.

✉ Alberto Cacciola
alberto.cacciola0@gmail.com

[1] Department of Biomedical, Dental Sciences and Morphological and Functional Images, University of Messina, 98125 Messina, Italy

[2] IRCCS Centro Neurolesi "Bonino Pulejo", S.S. 113, Via Palermo, C.da Casazza, 98124 Messina, Italy

[3] Department of Clinical and Experimental Medicine, University of Messina, 98125 Messina, Italy

Keywords Cerebellum · Connectivity · CSD · Limbic system · Mammillary bodies · Tractography

Introduction

Traditionally, cerebellar physiological function has long been confined to its motor control features; however, it has now become evident that the cerebellum plays a crucial role for many non-somatic functions other than the coordination of movement, and is engaged also in the regulation of cognition and emotion [1–6].

The best clinical evidence in humans, supporting the role of the cerebellum in non-somatic functions, is the cerebellar cognitive affective syndrome [6].

This syndrome, which occurs following lesions of the cerebellar posterior lobe but not the anterior lobe, is characterized by a range of executive, autonomic, visuospatial, linguistic, and affective deficits.

This constellation of non-somatic symptoms has also been reported in subsequent studies in adults and children, and the observation that the syndrome results from lesions of the cerebellar posterior lobe has also withstood scrutiny [7–14].

Interestingly, CCAS may occur in the absence of motor impairment corroborating the concept of a sensorimotor-cognitive anatomo-functional dichotomy in cerebellar organization [14–17].

Unfortunately, in contrast to the well-known regional cerebellar anatomy for motor control [18, for review], the anatomical connectivity underlying cerebellar modulation of cognition and emotion remains unclear.

In addition to corticopontine afferents from motor and non-motor regions, the cerebellum also receives inputs from the medial mammillary bodies, engaged in memory [19, 20], and multimodal deep layers of the superior colliculus.

🐑 Springer

Moreover, the cerebellum has reciprocal connections with the hypothalamus [20, 21] and with brainstem areas (ventral tegmental area, periaqueductal gray, and locus coeruleus) that are connected with limbic and paralimbic regions [22].

In terms of functional cerebello-hypothalamic connectivity, several authors showed that electrical stimulation of the cerebellum produced evoked responses in the amygdala and hippocampus and altered abnormal discharges in the latter [23, 24]. Furthermore, Moruzzi [25] showed that stimulation of the cerebellum altered the phenomenon of sham rage derived from hypothalamic stimulation [25, 26], suggesting that the cerebellum may act on behavioral responses belonging to complex autonomic reaction.

In line with this hypothesis, Snider showed the presence of anatomical projections from the fastigial nucleus to the hypothalamus [27]. Hereafter, many other authors provided evidence of interconnections between the cerebellum, hypothalamus, and limbic system [27–30].

Interestingly, anatomical and physiological evidences have now identified vermis as the principal target of such limbic connections [3, 31, 32].

Indeed, stimulation of the cerebellar vermis modulates firing patterns in the hippocampus, amygdala, and septum [33–35] and it can ameliorate aggression [36].

In a previous diffusion tensor imaging (DTI) study, we found the existence of a direct cerebello-limbic connection between the vermis; cerebellar lobules VIII, IX, X, crus I, and crus II; and the hippocampus, thus providing a new anatomical framework for the comprehension of the non-somatic cerebellar functions [37].

DTI is a MRI technique that allows to visualize in vivo white matter fibers, estimating properties of preferential anisotropic diffusion of magnetically labeled water into myelinated axons [38, 39]. Constrained spherical deconvolution (CSD) is a robust diffusion modeling technique which allows to overcome some of the most important limitations of the DTI approach, such as partial volume effect and the inability to resolve complex fiber configurations within a single voxel [40, 41]. Using this technique, we were able to reconstruct a limbic, basal ganglia, and cerebellum connectome in both normal and pathological conditions [37, 42–46].

In the present paper, we would like to further extend our previous work on cerebello-limbic pathways by evaluating the connectivity between the cerebellum and hypothalamus using CSD tractography. We hypothesized that the cerebellum may receive limbic inputs from the mammillary bodies and/or may give an output to the hypothalamus, thus influencing autonomic functions, visuospatial orientation, and memory functions. The results of this study could improve our understanding of non-motor cerebellar functions and may shed new light on several diseases where clinically relevant impairments in navigational skills or memory may become manifest at early stages of the disease.

Materials and Methods

Subjects

We recruited 13 healthy humans with no history of any overt neurological or psychiatric diseases. The research followed the tenets of the Declaration of Helsinki; written informed consent was obtained from all included subjects, after explanation of the nature and possible consequences of the procedure. The study was approved by the institutional review board of IRCCS Bonino Pulejo, Messina, Italy (Scientific Institute for Research, Hospitalization and Health Care), protocol number 15/2012.

Data Acquisition

We performed the following MRI sequences with a 3T Achieva Philips scanner using a 32-channel SENSE head coil:

1. Three-dimensional high-resolution T1-weighted fast field echo (FFE) sequence was acquired using the following parameters: repetition time (TR) = 25 ms, echo time (TE) = 4.6 ms, flip angle = 30°, field of view (FOV) = 240 × 240 = mm^2, reconstruction matrix = 240 × 240 voxel, voxel size = 1 × 1 × 1 mm, and slice thickness = 1 mm.
2. Three-dimensional high-resolution T2-weighted turbo spin echo (TSE) sequence was obtained using the following parameters: TR = 2500 ms, TE = 380 ms, FOV = 250 × 250 mm^2, reconstruction matrix = 312 × 312 voxel, voxel size = 0.8 × 0.8 × 0.8 mm, and slice thickness = 0.8 mm.
3. A dual-phase encoded pulsed gradient spin echo diffusion-weighted sequence [47] using 60 gradient diffusion directions was chosen following an electrostatic repulsion model [48]. The other sequence parameters were as follows: diffusion-weighting b-factor = 1000 s/mm^2, TR = 11,884 ms, TE = 54 ms, FOV = 240 × 240 mm^2, reconstruction matrix = 120 × 120 voxel, in-plane voxel size = 2 × 2 mm^2, axial slice thickness = 2 mm, and no interslice gap.

Preprocessing and Coregistration

SPM8 MATLAB tool (http://www.fil.ion.ucl.ac.uk/spm/software/spm8/) was used to correct diffusion images for motion as well as for eddy currents distortion artifacts; a rotational part of transformations was later applied to individual gradient directions. High-resolution T1 and T2 images were then coregistered to preprocessed DWIs using a pipeline outlined in [49] and used in our previous work [44]. In brief, using new segment option of SPM8, we

extracted cerebrospinal fluid (CSF) component probability masks from b0 image and structural scans. CSFs of structural scans were subsequently warped to match the CSF estimated from the b0 image using FLIRT and FNIRT FSL utilities (http://fsl.fmrib.ox.ac.uk/fsl/fslwiki/). Estimated warping fields were eventually applied to structural scans. Thanks to abovementioned workflow we were able to align structural scans onto diffusion images with high precision, thus reducing possible misalignment biases coming from usage, in diffusion images' space, of region of interest (ROI) segmented in space of structural scans.

Segmentation

On T1-weighted images, segmentation of the mammillary bodies was manually performed by a skilled neuroradiologist as follows: firstly, the individual volumes obtained from the 3D T1-weighted FFE sequence were loaded into the viewer; secondly, the contrast values in the viewer were set to maximally increase the visibility of the areas; thirdly, the axial view was zoomed to facilitate the drawing of the mammillary bodies mask; and fourthly, the mammillary bodies were visualized in coronal and sagittal views to better define it.

The segmentation of the dentate nucleus was manually performed on T2-weighted TSE images, which permitted to obtain high-resolution images with a relatively short acquisition time. At the same time, this sequence allowed to obtain a fine representation of the iron-loaded nuclei due to a T2* effect linked with the use of a very long echo time. The right and left dentate nuclei were depicted as hypointense bean-shaped structures and were traced individually on axial slices of the coregistered MR images and then saved as ROIs using the viewer provided with the MRtrix3 software.

In addition, we segmented the substantia nigra and red nucleus bilaterally to be set as regions of avoidance (ROAs).

Volumetric segmentation of the cerebellum was performed on the coregistered T1 images with the FreeSurfer image analysis suite by using the Desikan-Killiany atlas, which is documented and freely available for download online (http://surfer.nmr.mgh.harvard.edu/). Successively, the segmentations obtained from each individual were visually inspected and, if needed, manually edited.

Tractography

We modeled diffusion signal by using a modified high angular resolution diffusion imaging (HARDI) technique, namely non-negative CSD, that is able to estimate the fiber orientation distribution function (fODF) directly from deconvolution of DW signal with a reference single-fiber response function [50]. Response function was estimated from the data on the basis of voxels having a fractional anisotropy (FA) index above 0.7, by using MRtrix software (http://jdtournier.

github.io/mrtrix-0.2/index.html). Probabilistic streamline fiber tracking was performed by calculating the fODF peak direction closest to the previous stepping direction using trilinear interpolation.

By using CSD, we were able to overcome the partial volume effects associated with DTI and also to improve, comparing with other types of HARDI acquisitions while discarding QBI (Q-balls imaging) and DSI due to long acquisition times required [38]. On the one hand, if higher b values permit to resolve smaller angles among fibers [50, 51], they increase the probability to find motion and eddy currents related artifacts due to longer acquisition times. For this reason, we preferred a lower b value in order to obtain the best quality speed trade-off.

We performed probabilistic CSD-based whole-brain tractography, using the following parameters: spherical harmonic degree = 8, step size = 0.2 mm, maximum angle = 10°, maximum fiber length = 150 mm, minimum fiber length = 40 mm, and minimal fODF amplitude = 0.15.

CSD combined with a probabilistic approach allows to track streamlines even in voxels with complex fiber geometries, though the number of false positive tends to increase. For this reason, we used a more conservative approach with respect to usual standards setting the minimal fODF amplitude = 0.15, thus keeping to a minimum false-positive fiber bundles. In this way, the tracking procedure involved only voxels with high probability to belong to the white matter [52, 53].

Before running tractography, we applied a small dilatation to WM masks in order to allow streamlines to reach our ROIs, placed in GM, for subsequent analyses. Target ROIs were moderately dilated to include gray/white matter boundaries, thus ensuring that streamlines were able to reach target ROIs for subsequent connectivity analysis.

For visualization purposes, we reconstructed a color-coded map in which red, blue, and green colors indicate the principal streamline directions [54]. Specifically, red color indicates a left–right pattern, green color an anterior–posterior pattern, and blue color a caudal–cranial pattern.

Connectivity Analysis

We extracted, for each subject, streamlines connecting the right and left mammillary bodies with inclusion masks. Connectivity was defined as the percentage of streamlines ending in each ROI (dentate nuclei and cerebellar cortices). Such numbers are used as markers of connectivity density, in both healthy and pathological conditions [55–58].

Since it is documented that streamlines are more likely to connect with larger ROIs or closer ROIs, we took these into account for volume and distance biases. Hence, we performed weighted connectivity defined as the density of the tracts connecting a couple of ROIs, scaling the number of

streamlines by the sum of inverse of the fiber length and the mean volume of two ROIs [59].

Statistical Analysis

Connectivity, FA, mean diffusivity (MD), axial diffusivity (AD), radial diffusivity (RD), and tract length mean are the parameters considered for each pathway. A non-parametric analysis was carried out because the results of the Shapiro-Wilk normality test indicated that most of the target variables were not normally distributed. The numerical data are presented in median and first–third quartiles for non-normal distributions. The Wilcoxon signed-rank test was used in order to compare, for each pathway (mammillary bodies-ipsilateral cerebellar cortex, mammillary bodies-contralateral cerebellar cortex, mammillary bodies-ipsilateral dentate nucleus, mammillary bodies-contralateral dentate nucleus), the results between the right and left sides (intra-pathway analysis) in each parameter. Spearman's rank correlation was used to assess whether there was a relationship between connectivity indices and other parameters. Analyses were performed using an open source R3.0 software package. A 95 % of confidence level was set with a 5 % alpha error. Statistical significance was set at $p < 0.05$.

Results

In total, 13 subjects (seven males and six females) were enrolled with a mean age of 35.46 ± 11 years.

In all subjects, we traced bilaterally fiber bundles connecting the cerebellum with the mammillary bodies. In particular, we isolated fiber bundles between the dentate nucleus and mammillary bodies, passing through the ipsilateral superior cerebellar peduncle (Fig. 1), ascending the medial mesencephalic tegmentum at the level of the inferior colliculi, surrounding the red nucleus, bending around the medial face of the substantia nigra, and finally reaching the mammillary body. Figure 2 shows in axial slices the anatomical course of the connections between the dentate nucleus and mammillary bodies. We identified both ipsilateral and contralateral components, the latter decussating at the level of midbrain (Fig. 3).

In addition, we found a less strong connectivity between the cerebellar cortex and the mammillary bodies. Starting our description from the cerebellum, these tracts originated in the anterior cerebellar cortex (vermis; lobules VIIB, VIIIA, VIIIB, X, crus I, and crus II), reached the medial part of the cerebellum, ascended the ipsilateral middle cerebellar peduncle, and finally reached the mammillary bodies (Fig. 4). Representation of the course of the connections between the cerebellum and mammillary bodies is depicted in axial slices in Fig. 5. Also for this pathway, we demonstrated the presence of both ipsilateral and contralateral connections, decussating at the level of the upper pons, as shown in Fig. 6.

Figure 7 reports the box plot of the pathway for each parameter. Intra-pathway analysis highlighted no significant differences for side factor in the pathway of each parameter ($p > 0.05$) (Table 1). A significant correlation between the left mammillary bodies-ipsilateral cerebellar cortex connectivity and RD ($r = -0.621$, $p = 0.026$) as well as a trend toward the correlation between the left mammillary bodies-

Fig. 1 Ipsilateral dentate nucleus-mammillary connections. Parasagittal views of left (*A*) and right (*B*) pathways connecting the dentate nucleus (*orange* Volume of Interest (VOI)) and ipsilateral mammillary body (*purple* VOI) via the superior cerebellar peduncle. The enlarged views better depict streamlines avoiding the substantia nigra (*cyan* VOI) and red nucleus (*red* VOI)
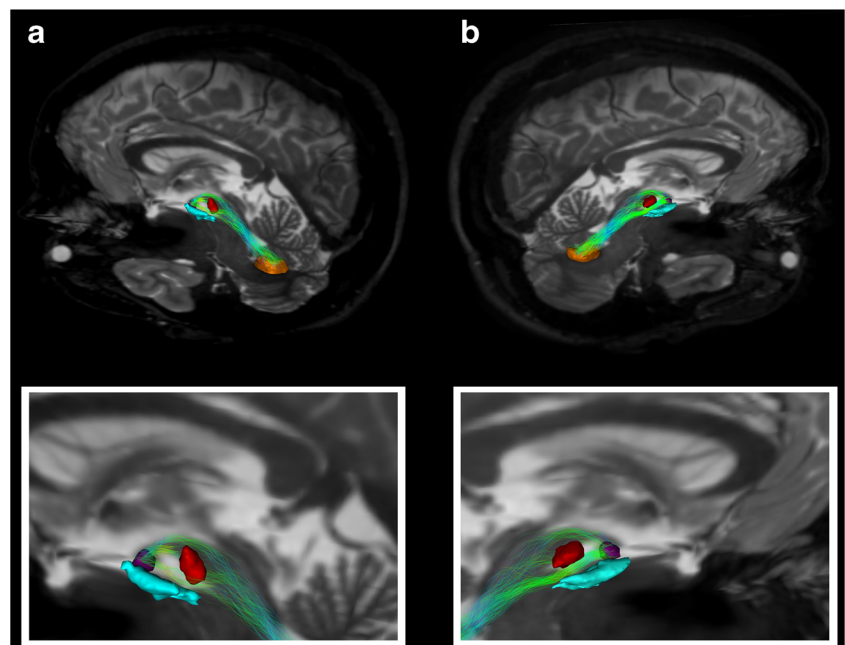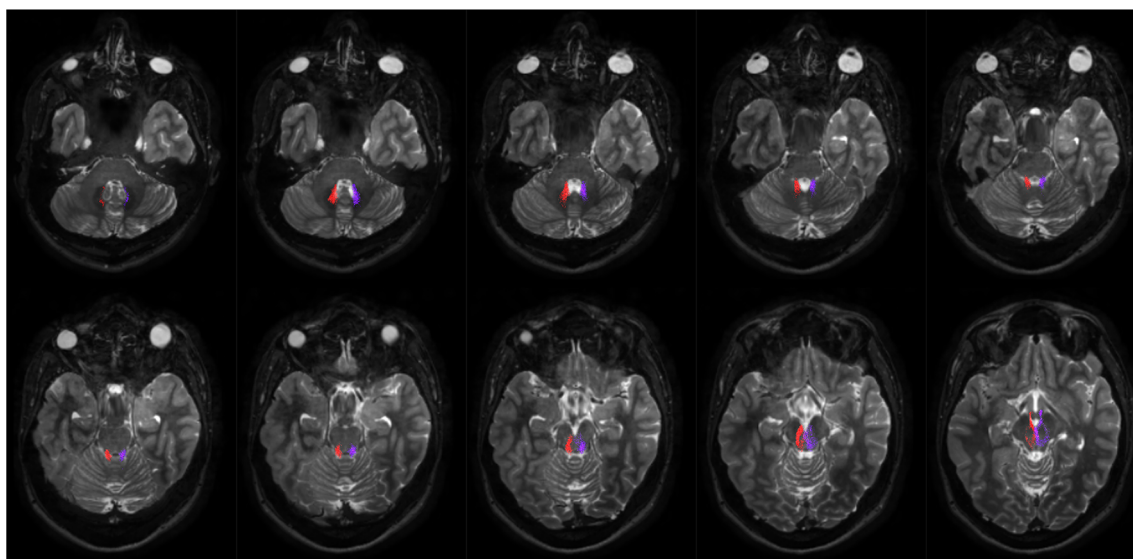
Fig. 2 Course of ipsilateral dentate nucleus-mammillary connections. Ten axial T2-weighted images show the course of the connections between the dentate nucleus and mammillary bodies. On the *right side*, fibers are *red* colored and, on the *left side*, *blue* colored. The *first three* *images* depict tracts leaving the dentate nuclei, and then fibers pass through the superior cerebellar peduncles, surround red nuclei, passing medially to the substantia nigra, and finally reach the mammillary bodies

contralateral dentate nucleus connectivity and FA ($r = -0.527$; $p = 0.067$) were observed (Fig. 8).

Discussion

In the present study, we showed the existence of connections between the mammillary bodies with both the cerebellar cortex and dentate nucleus in the human brain.

These findings are in line with previous studies performed in rodents and primates [60–62]. In particular, afferent connections from the lateral mammillary nucleus to vermis lobule IX (uvula) and the cerebellar anterior lobe in exemplars of three shrew (*Tupaia glis*) were reported, while no reciprocal efferent projections between the cerebellar cortex and cerebellar nuclei to the mammillary bodies were found [63]. Similar results have been reported in a prosimian primate (*Galago crassicaudatus*) [64]. Finally, studies performed on the squirrel monkey described a slightly different network, where hypothalamo-cerebellar fibers mainly reach lateral mammillary and supramammillary nuclei, connecting them with paraflocculus, dorsal paramedian lobule, and lobule V of the anterior lobe, while the ansiform lobule is reached by projecting fibers from medial mammillary and supramammillary nuclei. As described in previous experiments, these connections have both ipsilateral and contralateral components, with an ipsilateral preponderance with few sparse efferent connections arising from globose and fastigial nuclei directed to the contralateral medial mammillary nucleus [20]. Finally, a study focused on connections between the cerebellar nuclei and hypothalamus performed on *Macaca fascicularis* revealed that all the deep cerebellar nuclei (dentate, fastigial, globose, and emboliform
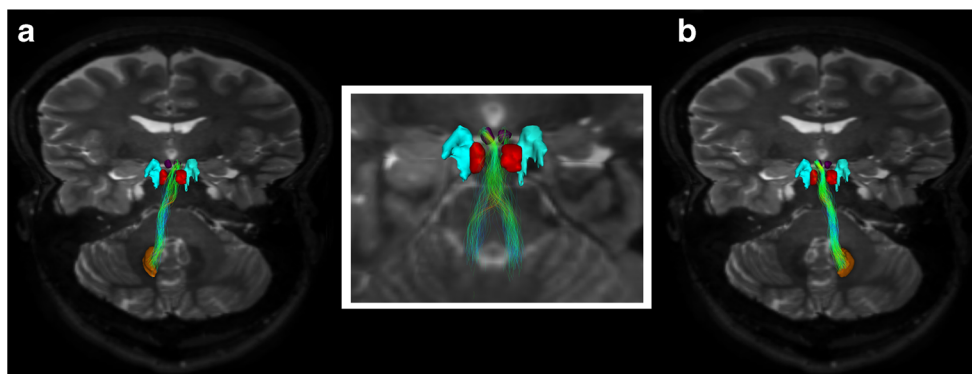

Fig. 3 Contralateral dentate nucleus-mammillary connections. *A* Representation in coronal view of the pathway connecting the right mammillary body (*purple* VOI) with contralateral dentate nucleus (*orange* VOI). *B* Coronal view shows the connection between the left mammillary body (*purple* VOI) and contralateral dentate nucleus (*orange* VOI). The *inset* in mid position focuses on the fibers exiting the superior cerebellar peduncles and decussating at the level of midbrain, below, and medially to red nuclei (*red* VOIs)

Fig. 4 Ipsilateral cerebellar cortex-mammillary connections. Parasagittal views of left (*A*) and right (*B*) pathways connecting the cerebellar cortex and ipsilateral mammillary body (*purple* VOI) via the middle cerebellar peduncle. In this case, fibers avoid the dentate nucleus (*orange* VOI). The enlarged views better depict streamlines avoiding the substantia nigra (*cyan* VOI) and red nucleus (*red* VOI)
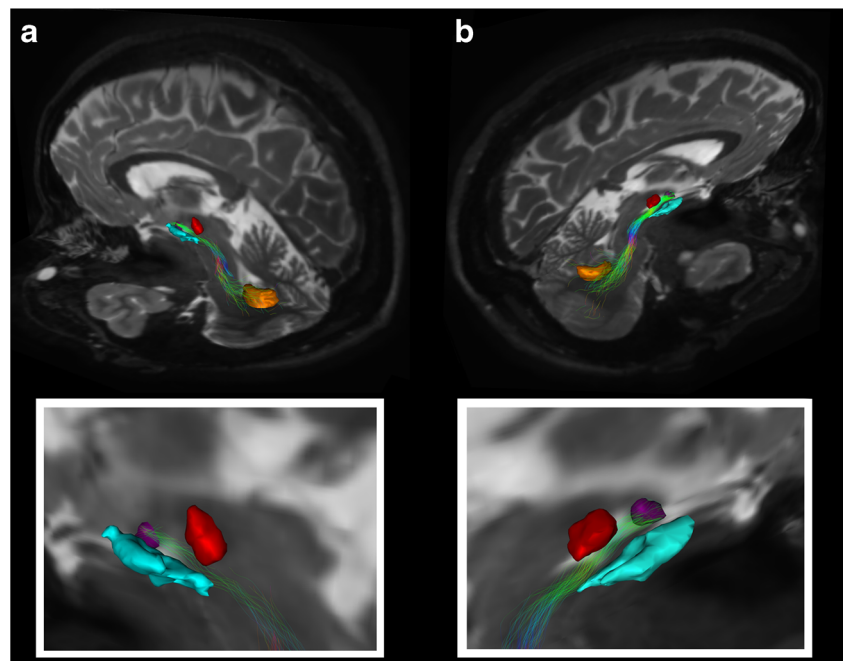
nuclei) received afferents from lateral and medial mammillary, supramammillary, and tuberomammillary nuclei; on the other hand, no significant efferent projections to the mammillary bodies were reported [65]. Pooling together the literature, it looks like that there is a predominant hypothalamic-cerebellar direction. A comparison between data from studies in animals and our data is shown in Table 2.

In the present study, we found that the mammillary bodies have a strong connectivity with the dentate nucleus and a less strong connectivity with the cerebellar cortex. In particular, fibers terminated in lobules VI, VII, VIII, crus I, and crus II and vermis in the posterior part of the cerebellum.

This is in line with the physiological view of a functional compartmentalization of the cerebellar cortex where the anterior lobe is related to sensorimotor functions while the posterior lobe (in particular, lobules VI and VII) may have a predominant cognitive function, and the posterior vermis may be involved in affective processes [66].
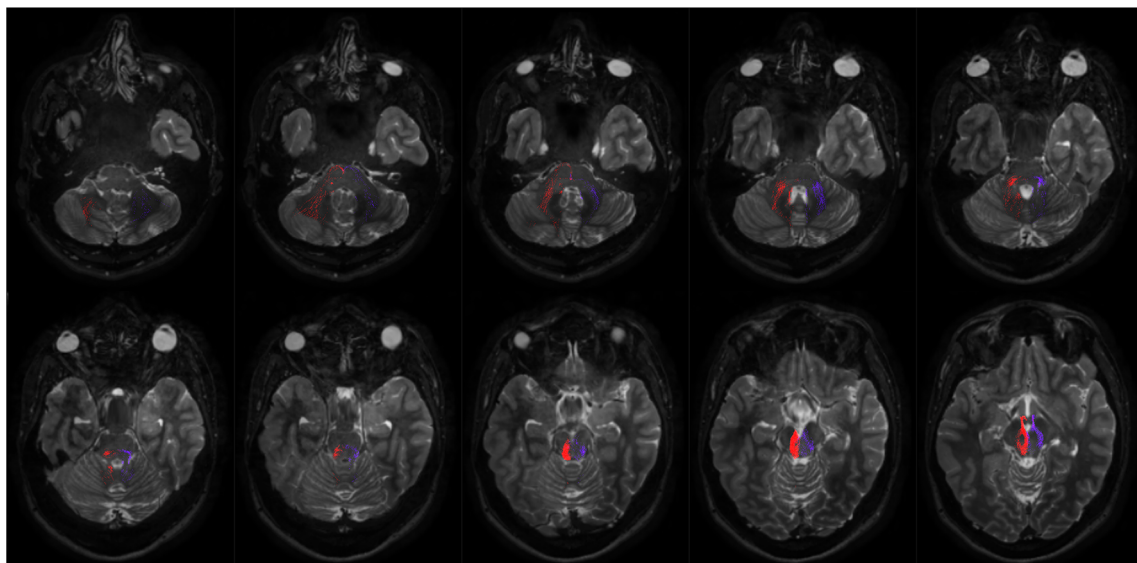

Fig. 5 Course of ipsilateral cerebellar cortex-mammillary connections. Ten axial T2-weighted images show the course of the connections between the cerebellar cortex and mammillary bodies. On the *right side*, fibers are *red* colored and, on the *left side*, *blue* colored. The *first row* shows streamlines leaving the cerebellar cortex and passing through the middle cerebellar peduncles. In the *second row*, at the level of midbrain, fibers encircle red nuclei, pass medially to the substantia nigra, and finally reach the mammillary bodies
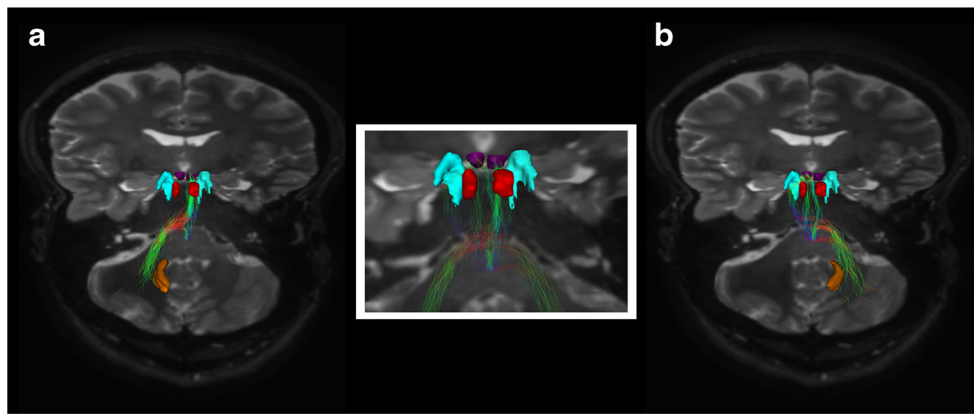
Fig. 6 Contralateral cerebellar cortex-mammillary connections. *A* Coronal view shows the connection between the right mammillary body (*purple* VOI) and contralateral cerebellar cortex, decussating at the level of the pons. *B* Coronal view shows the connection between the left mammillary body (*purple* VOI) and right cerebellar cortex, decussating at the level of the pons. Note that these pathways also run externally to dentate nucleus (*orange* VOI). The enlarged view magnifies streamlines crossing the midline at the level of the pons and bypassing the red nuclei (*red* VOIs) and substantia nigra (*cyan* VOIs)
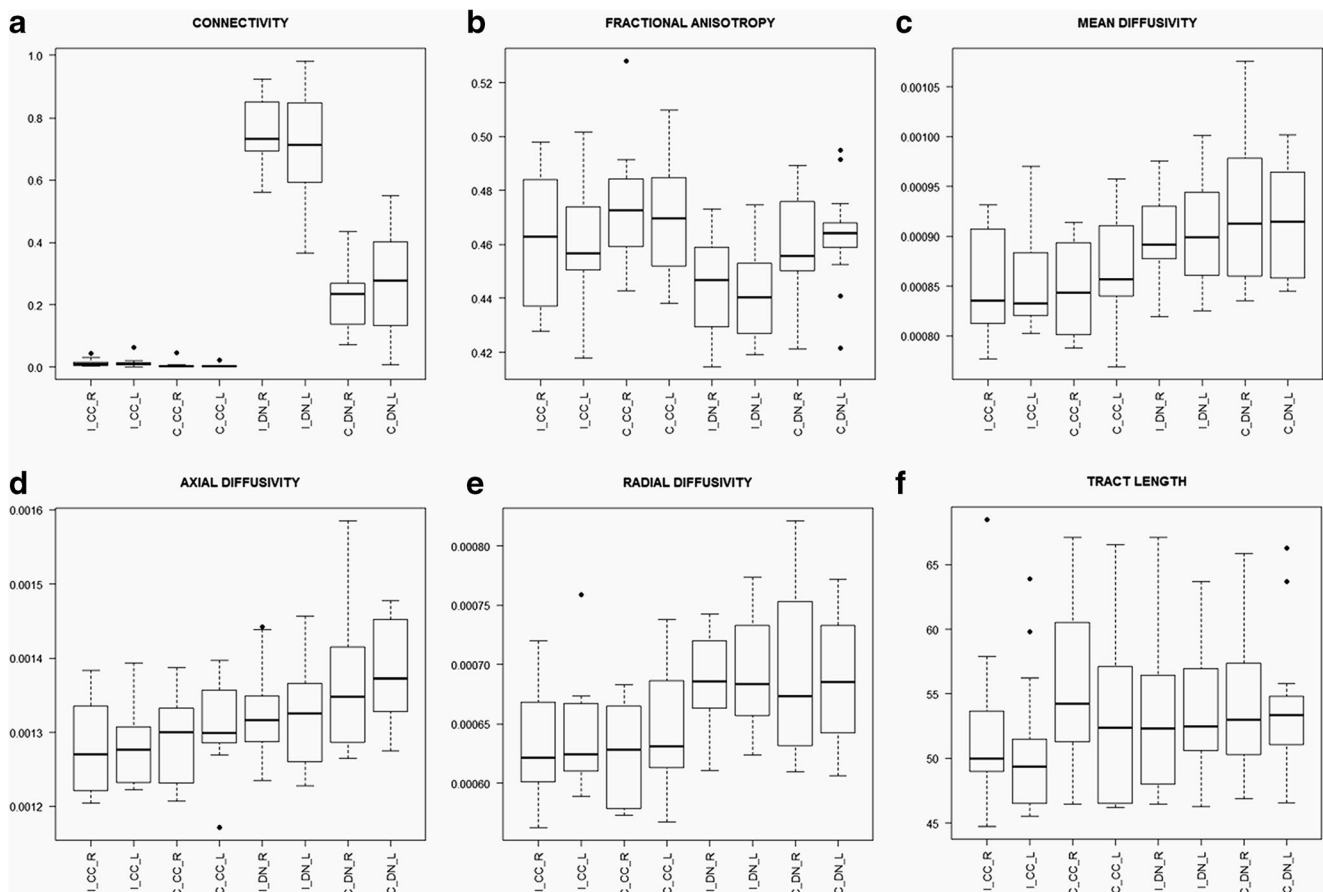

Fig. 7 Representation by box plot of parameters for each pathway in the right and left sides: **a** connectivity, **b** fractional anisotropy, **c** mean diffusivity, **d** axial diffusivity, **e** radial diffusivity, and **f** tract length mean. *I_CC_R* right mammillary bodies-ipsilateral cerebellar cortex, *I_CC_L* left mammillary bodies-ipsilateral cerebellar cortex, *C_CC_R* right mammillary bodies-contrala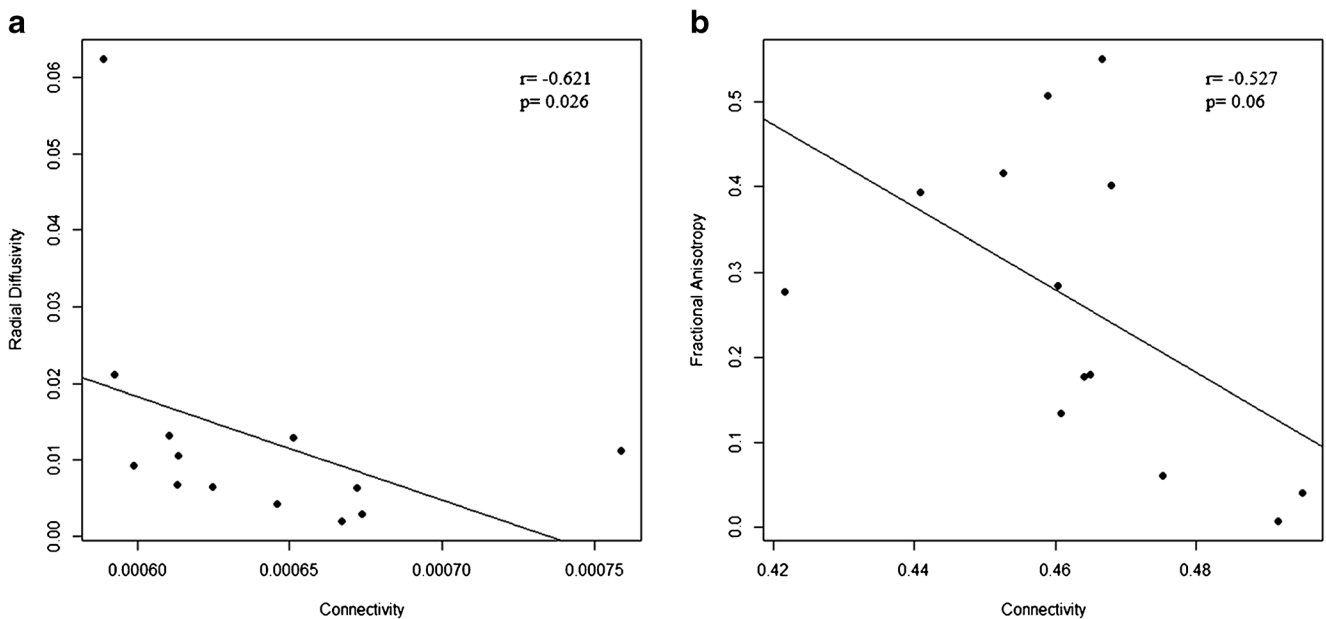teral cerebellar cortex, *C_CC_L* left mammillary bodies-contralateral cerebellar cortex, *I_DN_R* right mammillary bodies-ipsilateral dentate nucleus, *I_DN_L* left mammillary bodies-ipsilateral dentate nucleus, *C_DN_R* right mammillary bodies-contralateral dentate nucleus, *C_DN_L* left mammillary bodies-contralateral dentate nucleus

Table 1 Intra-pathway differences of pathway values in the right and left sides

	Median (I–III quartiles)					
	Connectivity	FA	MD	AD	RD	Tract length
Mammillary body-ipsilateral cerebellar cortex						
Right	0.009 (0.005–0.016)	0.463 (0.437–0.484)	0.0008 (0.0008–0.0009)	0.0013 (0.0012–0.0013)	0.0006 (0.0006–0.0007)	49.973 (48.988–53.649)
Left	0.009 (0.006–0.013)	0.457 (0.451–0.474)	0.0008 (0.0008–0.0009)	0.0013 (0.0012–0.0013)	0.0006 (0.0006–0.0007)	49.349 (46.518–51.505)
p value[a]	0.588	0.893	0.839	0.946	0.787	0.588
Mammillary body-contralateral cerebellar cortex						
Right	0.002 (0.002–0.005)	0.473 (0.459–0.484)	0.0008 (0.0008–0.0009)	0.0013 (0.0012–0.0013)	0.0006 (0.0006–0.0007)	54.26 (51.258–60.508)
Left	0.003 (0.0008–0.005)	0.470 (0.452–0.485)	0.0008 (0.0008–0.0009)	0.0013 (0.0013–0.0014)	0.0006 (0.0006–0.0007)	52.396 (46.505–57.109)
p value[a]	0.376	0.735	0.340	0.414	0.414	0.273
Mammillary body-ipsilateral dentate nucleus						
Right	0.732 (0.694–0.850)	0.447 (0.429–0.459)	0.0009 (0.0008–0.0009)	0.0013 (0.0013–0.0013)	0.0007 (0.0006–0.0007)	52.3 (47.989–56.412)
Left	0.714 (0.594–0.849)	0.440 (0.427–0.453)	0.0009 (0.0008–0.0009)	0.0013 (0.0013–0.0014)	0.0007 (0.0006–0.0007)	52.451 (50.590–56.941)
p value[a]	1	0.340	0.839	0.787	0.735	1
Mammillary body-contralateral dentate nucleus						
Right	0.236 (0.138–0.270)	0.456 (0.450–0.476)	0.0009 (0.0008–0.0010)	0.0013 (0.0013–0.0014)	0.0007 (0.0006–0.0007)	53.05 (50.318–57.362)
Left	0.277 (0.134–0.402)	0.464 (0.459–0.468)	0.0009 (0.0008–0.0009)	0.0014 (0.0013–0.0014)	0.0007 (0.0006–0.0007)	53.382 (51.049–54.836)
p value[a]	0.893	0.497	0.946	0.839	0.839	0.273

[a] Wilcoxon signed-rank test

FA fractional anisotropy, *MD* mean diffusivity, *AD* axial diffusivity, *RD* radial diffusivity

Fig. 8 Significant correlation between the connectivity and diffusion parameters. **a** Scatter plot of connectivity and radial diffusivity for mammillary-ipsilateral cerebellar cortex pathway in the left side. **b** Scatter plot of connectivity and fractional anisotropy for left mammillary-contralateral dentate nucleus pathway

Table 2 Overview of cerebellar-mammillary connections in animals

	Cat [19]	Three shrew (Tupaia glis) [63]	Greater bushbaby (Galago crassicaudatus) [64]	Squirrel monkey (Saimiri sciureus) [29, 62]	Macaca fascicularis [65]	Humans
Cerebellar cortical regions	Anterior lobe vermal and intermediate cortex (lobules IV and V), posterior lobe vermis, (lobule VII), lobulus simplex, crus I, crus II, paramedian lobule	Vermis lobule IX (uvula); anterior lobule V	Lobule V; lobule VI; vermal lobule V; vermal lobule VII; paraflocculus; paramedian lobule	Paraflocculus; dorsal paramedian lobule; lobule V of the anterior lobe; ansiform lobule	Unknown	Posterior lobule VI; posterior lobule VII; posterior lobule VIII; crus I, crus II, posterior vermis
Cerebellar deep nuclei	Unknown	Unknown	Dentate nucleus; globose (anterior interposed) nucleus	Globose nucleus; fastigial nucleus	Dentate nucleus; globose nucleus; emboliform nucleus; fastigial nucleus	Dentate nucleus
Mammillary nuclei	Tuberomammillary nucleus; lateral mammillary nucleus	Lateral mammillary nucleus	Tuberomammillary nucleus; lateral mammillary nucleus	Medial mammillary nucleus (to ansiform lobule and to deep nuclei); lateral mammillary nucleus (to other cortical regions) supramammillary nucleus (to all cortical regions)	Lateral mammillary nucleus; medial mammillary nucleus; supramammillary nucleus; tuberomammillary nucleus	Unknown
Connection type	Bilateral with ipsilateral preponderance	Bilateral with ipsilateral preponderance	Bilateral	Bilateral with ipsilateral preponderance (to the cortex); contralateral (to nuclei)	Bilateral with ipsilateral preponderance	Bilateral with ipsilateral preponderance

The existence of these parallel distinct networks may explain why in patients with cerebellar lesions cognitive and affective symptoms can even occur in the absence of motor symptoms [67–69].

The hypothesis of an "emotional" cerebellum involving posterior vermian and paravermian regions is also suggested by functional neuroimaging studies that have shown a significant posterior cerebellar activation during recognition of (i) facial emotions [70], (ii) pleasant vs unpleasant visual stimuli [71], (iii) subjective mood of sadness and anxiety [72, 73], (iv) positive mood states [74], and (v) fear conditioning and fear learning [75].

Physiological Relevance of Cerebellar-Hypothalamic Connectivity

Despite we cannot establish the directionality of cerebellar-mammillary connections, the present work may open a window to some physiological speculations.

It can be hypothesized that the cerebellum may receive limbic inputs from the mammillary bodies and/or may give an output to the hypothalamus, thus influencing vegetative and memory functions.

The involvement of the cerebellum in regulating autonomic functions has been reported in many animal studies (control of blood pressure [76], control of visceral, vegetative, and immune functions, reviewed in [77]). On the other hand, the role of the cerebellum on autonomic functions, in humans, is still a matter of debates, although some data are now emerging.

For instance, Schmahmann et al. reported that hunger significantly increased the regional cerebral blood flow (rCBF) in a number of brain regions of human subjects including the hypothalamus, limbic structures, as well as bilateral lobule V of the cerebellar cortex in the paravermian regions [78]. In addition, in a functional magnetic resonance imaging (fMRI) study, the cerebellum, supplementary motor area, somatosensory cortex, anterior cingulate, and orbitofrontal cortices were activated in a minute after glucose acquisition through a per-oral rubber tube [79].

In line with a role of the cerebellum on autonomic functions, it was shown that a fear-conditioned heart rate increase was impaired in patients with medial cerebellar lesions [80]. It has been postulated that direct cerebello-hypothalamic projections may modulate cardiovascular regulation by acting on brainstem neurons sensitive to baroreflex and osmotic pressure [81].

Regarding emotion and cognition, Reiman et al. revealed an activation in lateral parts of both cerebellar hemispheres (lobule VI) as well as in the other central structures subserving emotional expression such as the hypothalamus, amygdala, hippocampus, and occipito-temporo-parietal and anterior temporal cortices, in human subjects passively viewing film clips that generated feelings of happiness, sadness, or disgust [82]. Moreover, several authors reported that the cerebellum is implicated in sensory, emotional, attentional, and cognitive processes independently from motor involvement [83–86].

Relevance of Cerebello-Mammillary Connections on Visuospatial Orientation and Memory

Clinical evidences in patients with cerebellar lesions indicated that visuospatial ability was impaired in patients with cerebellar damage [87].

This notion is supported from recent neuroimaging data showing cerebellar activation during simple spatial tasks such as line bisection judgment [88] and during the mental rotation of objects [89].

In addition, cerebellar circuits play a pivotal role for acquisition of the procedural components required for spatial learning [90].

Neuroimaging findings in young individuals and lesion studies have identified a complicate network involved in human navigation, including the hippocampus, parahippocampal gyrus, cerebellum, parietal cortex, and retrosplenial cortex [91–93].

A specific role of the cerebellum in spatial navigation has been recently suggested by Rochefort and colleagues who hypothesized a direct pathway linking cerebellum and hippocampus [94].

In keeping with this hypothesis, we have recently demonstrated in normal humans, by using CSD tractography, the presence of a direct connection between the cerebellum (vermis; lobules VII, IX, X, crus I, and crus II; and fastigial nucleus) and the hippocampus [37].

Recent advances in our understanding of the mammillary bodies and their connections have shed new light on the possible role of these structures in high-order functions, such as spatial memory, thus challenging the prevalent hippocampal-centric view of mammillary body function and considering a wider network of structures interconnected with mammillary bodies [95]. In this perspective, a direct cerebello-mammillary pathway may be another piece of this complicate circuit implicated in visuospatial orientation.

Although the mammillary bodies have been implicated in amnesia perhaps for longer than any other single brain region, their role in memory has remained elusive.

This uncertainty persists despite the mammillary body pathology has been linked to the amnesic Korsakoff's syndrome [96]. Indeed, mammillary body damage is not sufficient alone to account for all of the memory deficits that are associated with Korsakoff's syndrome, considering that mammillary body degeneration is sometimes found in the absence of amnesia. On the other hand, it has been reported that anterior thalamic nucleus pathology was the best predictor of memory loss in patients with Korsakoff's syndrome, Wernicke's syndrome, and alcoholism [97, 98].

Limitations

It is known that tractography suffers from inherent technical limitations. First of all, tractography is not able to offer a direct

visualization of axons, whose diameter is typically less than 10 μm, but only a possible reconstruction of their trajectory according to local water diffusion anisotropy. Although our results are anatomically plausible compared with previous anatomical descriptions of these circuits, tractographic findings should be carefully considered and interpreted with caution. In the present work, we decided to use more conservative tracking criteria in respect to usual standard [44, 52, 99], at the cost of an underestimation issue, thus making our tractographic findings more reliable. Another important drawback of this technique is the lack of information regarding the directionality of the signal transmission [100, 101] and, therefore, whether the pathway that we revealed in the present study is hypothalamo-cerebellar, cerebello-hypothalamic, or reciprocal. Finally, tractography is unable to detect synapses and gap junctions, and thus, it does not allow to determine if a neural connection is mono- or polysynaptic. Therefore, further studies based on functional connectivity approach and postmortem microsurgery dissection and/or anterograde and retrograde tracer studies in animals are recommended in order to confirm definitively the existence of this pathway and to give more insights about its functions. Anyway, tractography still remains the only existing technique allowing to investigate neural connections in the human brain in vivo and non-invasively.

Conclusions

In conclusion, we demonstrated, in vivo, in humans, the presence of direct cerebello-mammillary connections in keeping with animal data, described in cats, rodents, and primates. These findings might be potentially useful to explore pathological conditions affecting cerebellar-limbic connections involved in autonomic functions, visuospatial orientation, and memory.

Compliance with Ethical Standards

Conflict of Interest   The authors declare that they have no conflict of interests.

References

1. Baillieux H, De Smet HJ, Paquier PF, De Deyn PP, Mariën P. Cerebellar neurocognition: insights into the bottom of the brain. Clin Neurol Neurosurg. 2008;110(8):763–73.

2. Leiner HC, Leiner AL, Dow RS. Does the cerebellum contribute to mental skills? Behav Neurosci. 1986;100(4):443–54.

3. Schmahmann JD. An emerging concept. The cerebellar contribution to higher function. Arch Neurol. 1991;48(11):1178–87.

4. Schmahmann JD. From movement to thought: anatomic substrates of the cerebellar contribution to cognitive processing. Hum Brain Mapp. 1996;4(3):174–98.

5. Schmahmann JD. Rediscovery of an early concept. Int Rev Neurobiol. 1997;41:3–27.

6. Schmahmann JD, Sherman JC. The cerebellar cognitive affective syndrome. Brain. 1998;121:561–79.

7. Exner C, Weniger G, Irle E. Cerebellar lesions in the PICA but not SCA territory impair cognition. Neurology. 2004;63(11):2132–5.

8. Levisohn L, Cronin-Golomb A, Schmahmann JD. Neuropsychological consequences of cerebellar tumour resection in children: cerebellar cognitive affective syndrome in a paediatric population. Brain. 2000;123:1041–50.

9. Molinari M, Petrosini L, Misciagna S, Leggio MG. Visuospatial abilities in cerebellar disorders. J Neurol Neurosurg Psychiatry. 2004;75(2):235–40.

10. Neau JP, Arroyo-Anllo E, Bonnaud V, Ingrand P, Gil R. Neuropsychological disturbances in cerebellar infarcts. Acta Neurol Scand. 2000;102(6):363–70.

11. Rapoport M, van Reekum R, Mayberg H. The role of the cerebellum in cognition and behavior: a selective review. J Neuropsychiatry Clin Neurosci. 2000;12(2):193–8.

12. Riva D, Giorgi C. The contribution of the cerebellum to mental and social functions in developmental age. Fiziol Cheloveka. 2000;26(1):27–31.

13. Schmahmann JD, Weilburg JB, Sherman JC. The neuropsychiatry of the cerebellum—insights from the clinic. Cerebellum. 2007;6(3):254–67.

14. Steinlin M, Imfeld S, Zulauf P, Boltshauser E, Lövblad KO, Ridolfi Lüthy A, Perrig W, Kaufmann F. Neuropsychological long-term sequelae after posterior fossa tumour resection during childhood. Brain. 2003;126(Pt 9):1998–2008.

15. Leggio MG, Silveri MC, Petrosini L, Molinari M. Phonological grouping is specifically affected in cerebellar patients: a verbal fluency study. J Neurol Neurosurg Psychiatry. 2000;69(1):102–6.

16. Fabbro F, Tavano A, Corti S, Bresolin N, De Fabritiis P, Borgatti R. Long-term neuropsychological deficits after cerebellar infarctions in two young adult twins. Neuropsychologia. 2004;42(4):536–45.

17. Manni E, Petrosini L. A century of cerebellar somatotopy: a debated representation. Nat Rev Neurosci. 2004;5(3):241–9.

18. Aas JE, Brodal P. Demonstration of topographically organized projections from the hypothalamus to the pontine nuclei: an experimental anatomical study in the cat. J Comp Neurol. 1988;268(3):313–28.

19. Haines DE, Dietrichs E. An HRP study of hypothalamo-cerebellar and cerebello-hypothalamic connections in squirrel monkey (Saimiri sciureus). J Comp Neurol. 1984;229(4):559–75.

20. Dietrichs E. Cerebellar autonomic function: direct hypothalamocerebellar pathway. Science. 1984;223(4636):591–3.

21. Snider RS, Maiti A. Cerebellar contributions to the Papez circuit. J Neurosci Res. 1976;2(2):133–46.

22. Heath RG, Harper JW. Ascending projections of the cerebellar fastigial nucleus to the hippocampus, amygdala, and other temporal lobe sites: evoked potential and histological studies in monkeys and cats. Exp Neurol. 1974;45(2):268–87.

23. Babb TL, Mitchell Jr AG, Crandall PH. Fastigiobulbar and dentatothalamic influences on hippocampal cobalt epilepsy in the cat. Electroencephalogr Clin Neurophysiol. 1974;36(2):141–54.

24. Moruzzi G. Sham rage and localized autonomic responses elicited by cerebellar stimulation in the acute thalamic cat. Proc XVII Internat Congress Physiol Oxford. 1947;1947:114–5.

25. Bard P. A diencephalic mechanism for the expression of rage with special reference to the sympathetic nervous system. Am J Phys. 1928;84:490–515.

26. Snider RS. Recent contribution to the anatomy and physiology of the cerebellum. Arch Neurol Psychiatr. 1950;64:196–219.

27. Anand BK, Malhotra CL, Singh B, Dua S. Cerebellar projections to limbic system. J Neurophysiol. 1959;22:451–7.

28. Dietrichs E, Haines DE. Observations on the cerebello-hypothalamic projection, with comments on non-somatic cerebellar circuits. Arch Ital Biol. 1985;123(2):133–9.

29. Supple Jr WF. Hypothalamic modulation of Purkinje cell activity in the anterior cerebellar vermis. Neuroreport. 1993;4(7):979–82.

30. Heath RG. Modulation of emotion with a brain pacemamer. Treatment for intractable psychiatric illness. J Nerv Ment Dis. 1977;165(5):300–17.

31. Schmahmann JD. The cerebrocerebellar system: anatomic substrates of the cerebellar contribution to cognition and emotion. Int Rev Psychiatry. 2001;13:247–60.

32. Berman AJ. Amelioration of aggression: response to selective cerebellar lesions in the rhesus monkey. In: Schmahmann JD, editor. The cerebellum and cognition. International review of neurobiology. Vol. 41. San Diego: Academic; 1997. p. 111–9.

33. Bobée S, Mariette E, Tremblay-Leveau H, Caston J. Effects of early midline cerebellar lesion on cognitive and emotional functions in the rat. Behav Brain Res. 2000;112(1–2):107–17.

34. Zanchetti A, Zoccolini A. Autonomic hypothalamic outbursts elicited by cerebellar stimulation. J Neurophysiol. 1954;17(5):475–83.

35. Heath RG, Dempesy CW, Fontana CJ, Myers WA. Cerebellar stimulation: effects on septal region, hippocampus, and amygdala of cats and rats. Biol Psychiatry. 1978;13(5):501–29.

36. Arrigo A, Mormina E, Anastasi GP, Gaeta M, Calamuneri A, Quartarone A, et al. Constrained spherical deconvolution analysis of the limbic network in human, with emphasis on a direct cerebello-limbic pathway. Front Hum Neurosci. 2014;8:987.

37. Basser PJ, Mattiello J, LeBihan D. MR diffusion tensor spectroscopy and imaging. Biophys J. 1994;66(1):259–67.

38. Henderson JM. "Connectomic surgery": diffusion tensor imaging (DTI) tractography as a targeting modality for surgical modulation of neural networks. Front Integr Neurosci. 2012;6:15.

39. Tournier JD, Yeh CH, Calamante F, Cho KH, Connelly A, Lin CP. Resolving crossing fibres using constrained spherical deconvolution: validation using diffusion-weighted imaging phantom data. NeuroImage. 2008;42(2):617–25.

40. Farquharson S, Tournier JD, Calamante F, Fabinyi G, Schneider-Kolsky M, Jackson GD, et al. White matter fiber tractography: why we need to move beyond DTI. J Neurosurg. 2013;118(6):1367–77.

41. Milardi D, Gaeta M, Marino S, Arrigo A, Vaccarino G, Mormina E, et al. Basal ganglia network by constrained spherical deconvolution: a possible cortico-pallidal pathway? Mov Disord. 2015;30:342–9.

42. Milardi D, Bramanti P, Milazzo C, Finocchio G, Arrigo A, Santoro G, et al. Cortical and subcortical connections of the human claustrum revealed in vivo by constrained spherical deconvolution tractography. Cereb Cortex. 2015;25:406–14.

43. Milardi D, Arrigo A, Anastasi G, Cacciola A, Marino S, Mormina E, et al. Extensive direct subcortical cerebellum-basal ganglia connections in human brain as revealed by constrained spherical deconvolution tractography. Front Neuroanat. 2016. doi:10.3389/fnana.2016.00029.

44. Mormina E, Arrigo A, Calamuneri A, Granata F, Quartarone A, Ghilardi MF, et al. Diffusion tensor imaging parameters' changes of cerebellar hemispheres in Parkinson's disease. Neuroradiology. 2015;57:327–34.

45. Milardi D, Cacciola A, Cutroneo G, Marino S, Irrera M, Cacciola G, Santoro G, Ciolli P, Anastasi G, Calabrò RS, Quartarone A. Red nucleus connectivity as revealed by constrained spherical deconvolution tractography. Neurosci Lett. 2016;626:68–73.

46. Embleton KV, Haroon HA, Morris DM, Ralph MA, Parker GJ. Distortion correction for diffusion-weighted MRI tractography and fMRI in the temporal lobes. Hu Brain Mapp. 2010;31:1570–87.

47. Jones DK, Horsfield MA, Simmons A. Optimal strategies for measuring diffusion in anisotropic systems by magnetic resonance imaging. Magn Reson Med. 1999;42:515–25.

48. Besson P, Dinkelacker V, Valabregue R, Thivard L, Leclerc X, Baulac M, et al. Structural connectivity differences in left and right temporal lobe epilepsy. NeuroImage. 2014;100:135–44.

49. Tournier JD, Calamante F, Connelly A. Robust determination of the fibre orientation distribution in diffusion MRI: non-negativity constrained super-resolved spherical deconvolution. NeuroImage. 2007;35:1459–72.

50. Alexander DC, Barker GJ. Optimal imaging parameters for fiber-orientation estimation in diffusion MRI. NeuroImage. 2005;27:357–67.

51. Descoteaux M, Deriche R, Knösche TR, Anwander A. Deterministic and probabilistic tractography based on complex fibre orientation distributions. IEEE Trans Med Imaging. 2009;28:269–86.

52. Tournier JD, Calamante F, Connelly A. Effect of step size on probabilistic streamlines: implications for the interpretation of connectivity analysis. Proc Intl Soc Mag Reson Med. 2011;19:2019.

53. Pajevic S, Pierpaoli C. Colour schemes to represent the orientation of anisotropic tissues from diffusion tensor data: application to white matter fiber tract mapping in the human brain. Magn Reson Med. 1999;42:526–40.

54. Smith RE, Tournier JD, Calamante F, Connelly A. SIFT: spherical-deconvolution informed filtering of tractograms. NeuroImage. 2013;67:298–312.

55. Behrens TE, Sporns O. Human connectomics. Curr Opin Neurobiol. 2012;22:144–53.

56. Bijttebier S, Caeyenberghs K, van den Ameele H, Achten E, Rujescu D, Titeca K, van Heeringen C. The vulnerability to suicidal behavior is associated with reduced connectivity strength. Front Hum Neurosci. 2015;9:632.

57. Li C, Huang B, Zhang R, Ma Q, Yang W, Wang L, et al. Impaired topological architecture of brain structural networks in idiopathic Parkinson's disease: a DTI study. Brain Imaging Behav 2016 [Epub ahead of print].

58. Cheng H, Wang Y, Sheng J, Kronenberger WG, Mathews VP, Hummer TA, Saykin AJ. Characteristics and variability of structural networks derived from diffusion tensor imaging. Neuroimag. 2012;61:1153–64.

59. Dietrichs E, Haines DE, Røste GK, Røste LS. Hypothalamocerebellar and cerebellohypothalamic projections—circuits for regulating nonsomatic cerebellar activity? Histol Histopathol. 1994;9(3):603–14.

60. Haines DE, Dietrichs E, Mihailoff GA, McDonald EF. The cerebellar-hypothalamic axis: basic circuits and clinical observations. Int Rev Neurobiol. 1997;41:83–107.

61. Haines DE, Dietrichs E. Evidence of an x zone in lobule V of the squirrel monkey (Saimiri sciureus) cerebellum: the distribution of corticonuclear fibers. Anat Embryol (Berl). 1991;184(3):255–68.

62. Haines DE, Sowa TE, Dietrichs E. Connections between the cerebellum and hypothalamus in the tree shrew (Tupaia glis). Brain Res. 1985;328(2):367–73.

63. Dietrichs E, Haines DE. Demonstration of hypothalamo-cerebellar and cerebello-hypothalamic fibres in a prosimian

primate (Galago crassicaudatus). Anat Embryol (Berl). 1984;170(3):313–8.

64. Haines DE, May PJ, Dietrichs E. Neuronal connections between the cerebellar nuclei and hypothalamus in Macaca fascicularis: cerebello-visceral circuits. J Comp Neurol. 1990;299(1):106–22.

65. Stoodley CJ, Schmahmann JD. Evidence for topographic organization in the cerebellum of motor control versus cognitive and affective processing. Cortex. 2010;46(7):831–44.

66. Paulus KS, Magnano I, Conti M, Galistu P, D'Onofrio M, Satta W, Aiello I. Pure post-stroke cerebellar cognitive affective syndrome: a case report. Neurol Sci. 2004;25(4):220–4.

67. Aarsen FK, Van Dongen HR, Paquier PF, Van Mourik M, Catsman-Berrevoets CE. Long-term sequelae in children after cerebellar astrocytoma surgery. Neurology. 2004;62(8):1311–6.

68. Gottwald B, Wilde B, Mihajlovic Z, Mehdorn HM. Evidence for distinct cognitive deficits after focal cerebellar lesions. J Neurol Neurosurg Psychiatry. 2004;75(11):1524–31.

69. George MS, Ketter TA, Post RM. SPECT and PET imaging in mood disorders. J Clin Psychiatry. 1993;54(Suppl):6–13.

70. Paradiso S, Robinson RG, Andreasen NC, Downhill JE, Davidson RJ, Kirchner PT, et al. Emotional activation of limbic circuitry in elderly normal subjects in a PET study. Am J Psychiatry. 1997;154(3):384–9.

71. Paradiso S, Robinson RG, Boles Ponto LL, Watkins GL, Hichwa RD. Regional cerebral blood flow changes during visually induced subjective sadness in healthy elderly persons. J Neuropsychiatry Clin Neurosci. 2003;15(1):35–44.

72. Liotti M, Mayberg HS, Brannan SK, McGinnis S, Jerabek P, Fox PT. Differential limbic–cortical correlates of sadness and anxiety in healthy subjects: implications for affective disorders. Biol Psychiatry. 2000;48(1):30–42.

73. Habel U, Klein M, Kellermann T, Shah NJ, Schneider F. Same or different? Neural correlates of happy and sad mood in healthy males. NeuroImage. 2005;26(1):206–14.

74. Lange I, Kasanova Z, Goossens L, Leibold N, De Zeeuw CI, van Amelsvoort T, Schruers K. The anatomy of fear learning in the cerebellum: a systematic meta-analysis. Neurosci Biobehav Rev. 2015;59:83–91.

75. Dow RS, Moruzzi G. The physiology and pathology of the cerebellum. Minneapolis: University of Minnesota Press; 1958.

76. Zhu JN, Yung WH, Kwok-Chong Chow B, Chan YS, Wang JJ. The cerebellar-hypothalamic circuits: potential pathways underlying cerebellar involvement in somatic-visceral integration. Brain Res Rev. 2006;52(1):93–106.

77. Schmahmann JD, Doyon J, McDonald D, Holmes C, Lavoie K, Hurwitz AS, et al. Three-dimensional MRI atlas of the human cerebellum in proportional stereotaxic space. NeuroImage. 1999;10:233–60.

78. Liu Y, Gao JH, Liu HL, Fox PT. The temporal response of the brain after eating revealed by functional MRI. Nature. 2000;405(6790):1058–62.

79. Maschke M, Schugens M, Kindsvater K, Drepper J, Kolb FP, Diener HC, Daum I, Timmann D. Fear conditioned changes of heart rate in patients with medial cerebellar lesions. J Neurol Neurosurg Psychiatry. 2002;72(1):116–8.

80. Wen YQ, Zhu JN, Zhang YP, Wang JJ. Cerebellar interpositus nuclear inputs impinge on paraventricular neurons of the hypothalamus in rats. Neurosci Lett. 2004;370(1):25–9.

81. Reiman EM, Lane RD, Ahern GL, Schwartz GE, Davidson RJ, Friston KJ, Yun LS, Chen K. Neuroanatomical correlates of externally and internally generated human emotion. Am J Psychiatry. 1997;154(7):918–25.

82. Gao JH, Parsons LM, Bower JM, Xiong J, Li J, Fox PT. Cerebellum implicated in sensory acquisition and discrimination rather than motor control. Science. 1996;272(5261):545–7.

83. Allen G, Buxton RB, Wong EC, Courchesne E. Attentional activation of the cerebellum independent of motor involvement. Science. 1997;275(5308):1940–3.

84. Parsons LM, Denton D, Egan G, McKinley M, Shade R, Lancaster J, Fox PT. Neuroimaging evidence implicating cerebellum in support of sensory/cognitive processes associated with thirst. Proc Natl Acad Sci U S A. 2000;97(5):2332–6.

85. Parsons LM, Egan G, Liotti M, Brannan S, Denton D, Shade R, et al. Neuroimaging evidence implicating cerebellum in the experience of hypercapnia and hunger for air. Proc Natl Acad Sci U S A. 2001;98(4):2041–6.

86. Schmahmann JD, Sherman JC. Cerebellar cognitive affective syndrome. Int Rev Neurobiol. 1997;41:433–40.

87. Fink GR, Marshall JC, Shah NJ, Weiss PH, Halligan PW, Grosse-Ruyken M, Ziemons K, Zilles K, Freund HJ. Line bisection judgments implicate right parietal cortex and cerebellum as assessed by fMRI. Neurology. 2000;54(6):1324–31.

88. Tagaris GA, Richter W, Kim SG, Pellizzer G, Andersen P, Ugurbil K, Georgopoulos AP. Functional magnetic resonance imaging of mental rotation and memory scanning: a multidimensional scaling analysis of brain activation patterns. Brain Res Brain Res Rev. 1998;26(2–3):106–12.

89. Petrosini L, Leggio MG, Molinari M. The cerebellum in the spatial problem solving: a co-star or a guest star? Prog Neurobiol. 1998;56(2):191–210.

90. Aguirre GK, Detre JA, Alsop DC, D'Esposito M. The parahippocampus subserves topographical learning in man. Cereb Cortex. 1996;6(6):823–9.

91. Katayama K, Takahashi N, Ogawara K, Hattori T. Pure topographical disorientation due to right posterior cingulate lesion. Cortex. 1999;35(2):279–82.

92. Maguire EA, Burgess N, Donnett JG, Frackowiak RS, Frith CD, O'Keefe J. Knowing where and getting there: a human navigation network. Science. 1998;280(5365):921–4.

93. Rochefort C, Lefort JM, Rondi-Reig L. The cerebellum: a new key structure in the navigation system. Front Neural Circuits. 2013;7:35.

94. Vann SD, Nelson AJ. The mammillary bodies and memory: more than a hippocampal relay. Prog Brain Res. 2015;219:163–85.

95. Davila MD, Shear P, Lane B, Sullivan EV, Pfefferbaum A. Mammillary body and cerebellar shrinkage in chronic alcoholics: an MRI and neuropsychological study. Neuropsychology. 1994;8:433–44.

96. Harding A, Halliday G, Caine D, Kril J. Degeneration of anterior thalamic nuclei differentiates alcoholics with amnesia. Brain. 2000;123(Pt1):141–54.

97. Cacciola A, Milardi D, Anastasi GP, Basile GA, Ciolli P, Irrera M, et al. A direct cortico-nigral pathway as revealed by constrained spherical deconvolution tractography in humans. Front Hum Neurosci. 2016;10:374.

98. Chung HW, Chou MC, Chen CY. Principles and limitations of computational algorithms in clinical diffusion tensor MR tractography. Am J Neuroradiol. 2011;32:3–13.

99. Mariën P, Saerens J, Nanhoe R, Moens E, Nagels G, Pickut BA, et al. Cerebellar induced aphasia: case report of cerebellar induced prefrontal aphasic language phenomena supported by SPECT findings. J Neurol Sci. 1996;144(1–2):34–43.

100. Gamper, E Zur Frage der Polioencephalitis der chronischen Alkoholiker. Anatomische Befunde beim chronischem Korsakow und ihre Beziehungen zum klinischen Bild. Deutsche Z. Nervenheilkd; 1928. pp. 122–129.

101. Parker GD, Marshall D, Rosin PL, Drage N, Richmond S, Jones DK. A pitfall in the reconstruction of fibre ODFs using spherical deconvolution of diffusion MRI data. NeuroImage. 2013;65:433–48.